Supplementary Information (SI) for Nanoscale.
This journal is © The Royal Society of Chemistry 2026

Supporting Information

Palladium-Based Polyelemental Nanoparticles for Ethanol Oxidation Reaction

Xiaoyu Hou,[a,†] Shiqi Yang,[a,†] Xianzhuo Lao,[a] Peng-Cheng Chen[a,*]

a College of Smart Materials and Future Energy, Fudan University, Shanghai 200438, China.

* Corresponding author. E-mail: pcchen@fudan.edu.cn

† These authors contributed equally to this work.

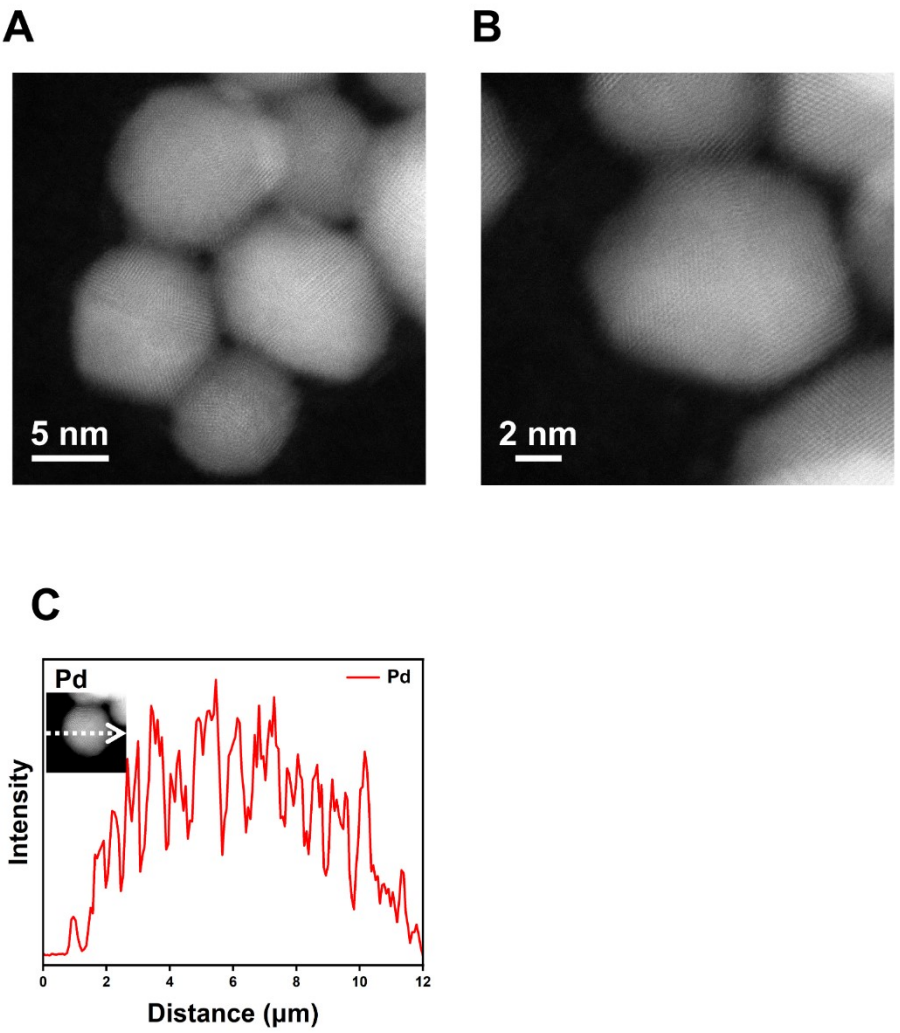

Figure S1. (A and B) HAADF-STEM images and (C) elemental line-scanning results of Pd nanoparticles.

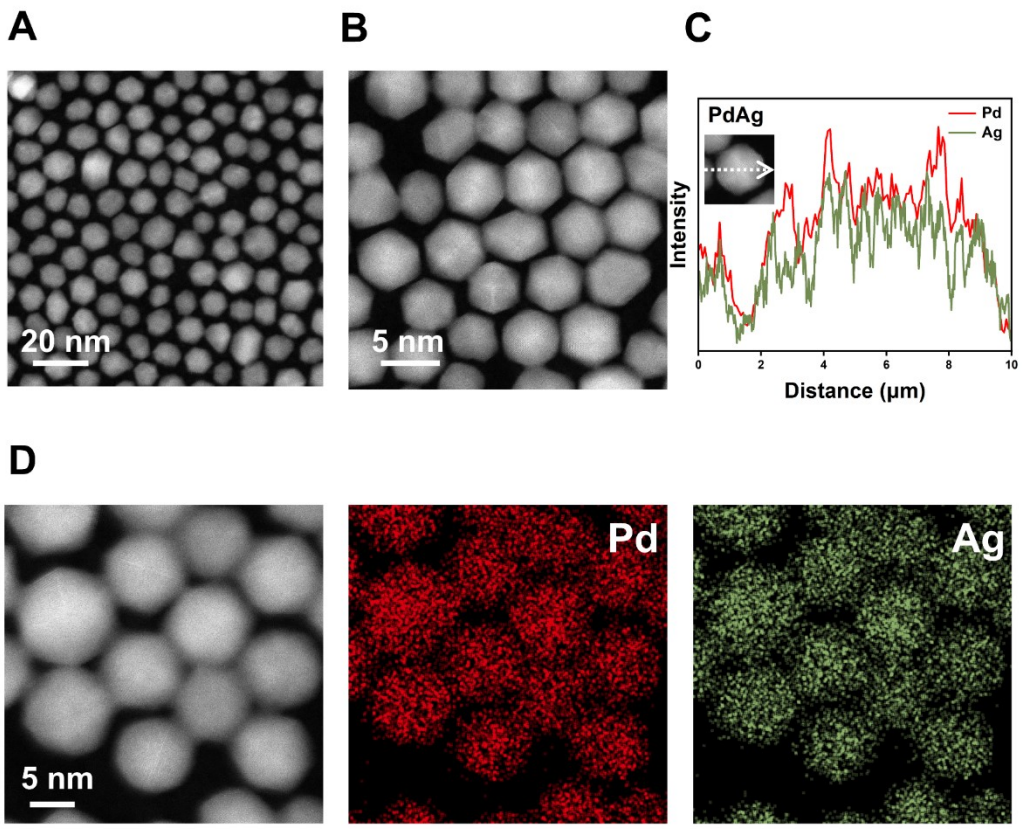

Figure S2. (A and B) HAADF-STEM images, (C) elemental line-scanning results, and (D) mapping of PdAg nanoparticles.

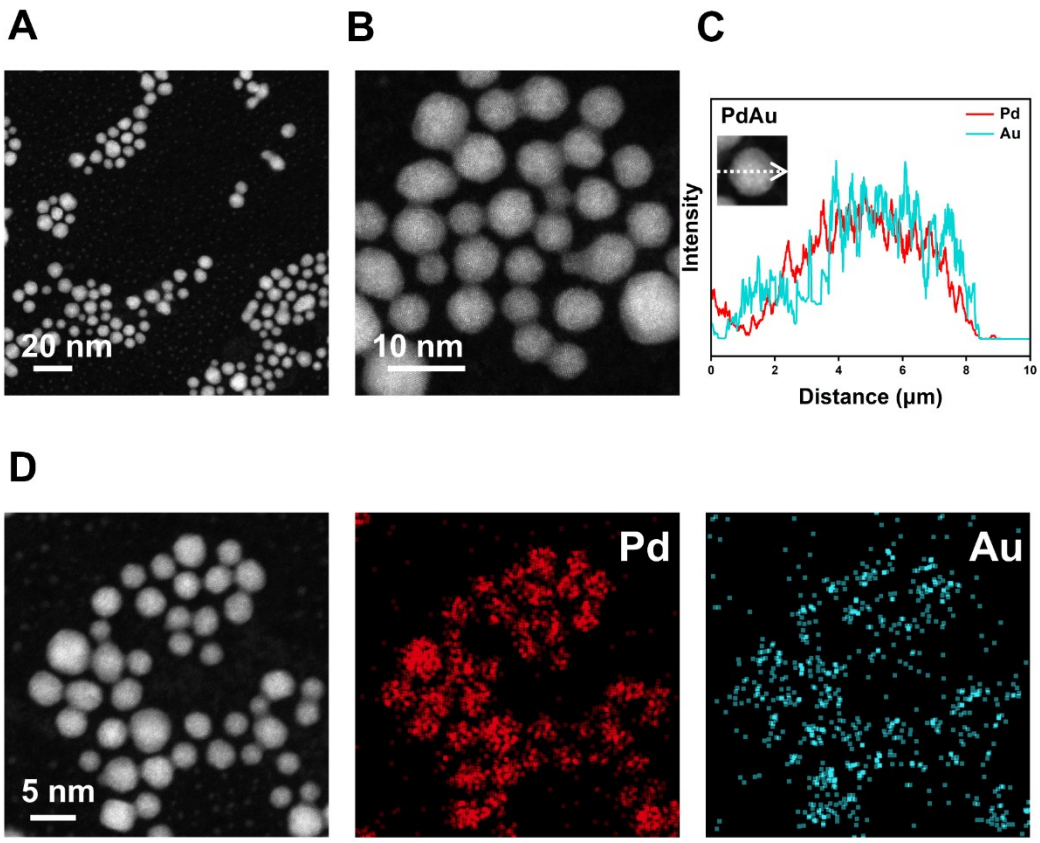

Figure S3. (A and B) HAADF-STEM images, (C) elemental line-scanning results, and (D) mapping of PdAu nanoparticles.

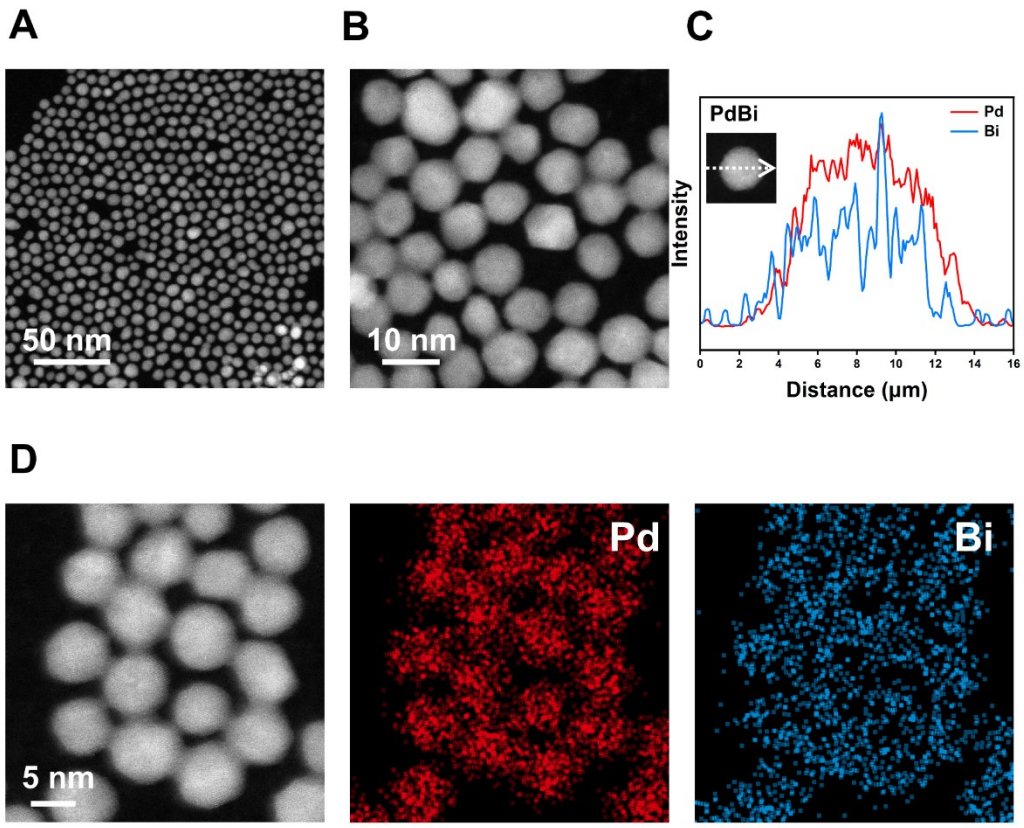

Figure S4. (A and B) HAADF-STEM images, (C) elemental line-scanning results, and (D) mapping of PdBi nanoparticles.

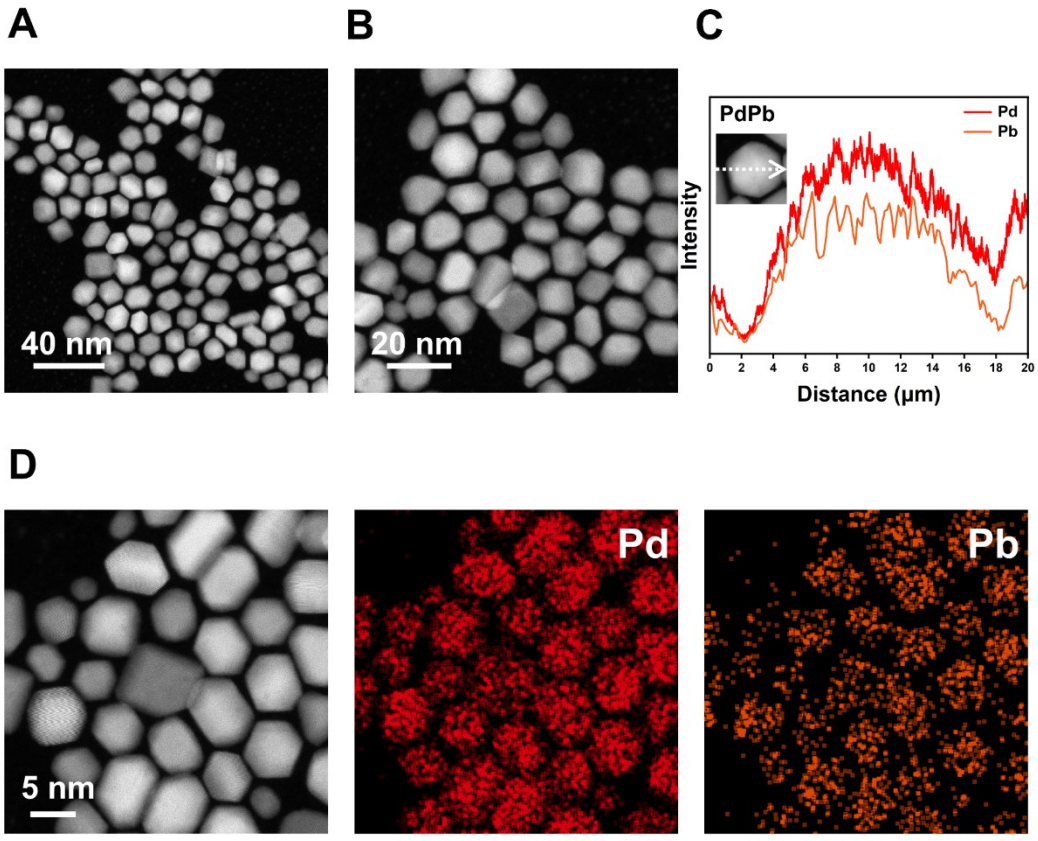

Figure S5. (A and B) HAADF-STEM images, (C) elemental line-scanning results, and (D) mapping of PdPb nanoparticles.

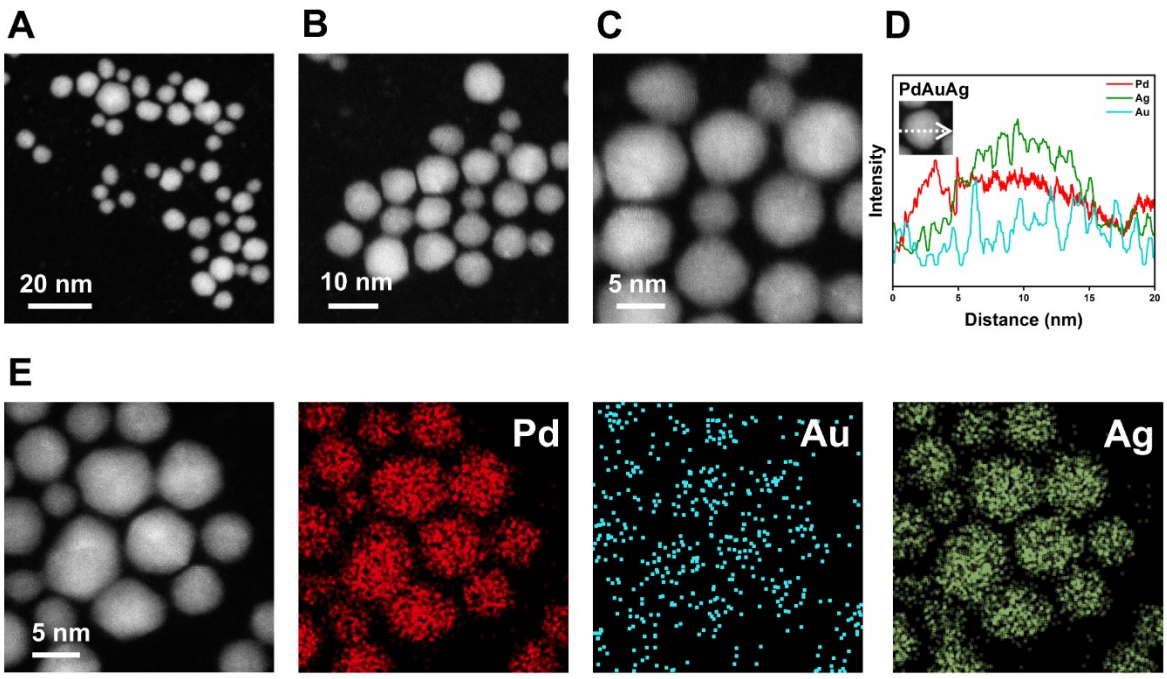

Figure S6. (A-C) HAADF-STEM images, (D) elemental line-scanning results, and (E) mapping of PdAuAg nanoparticles.

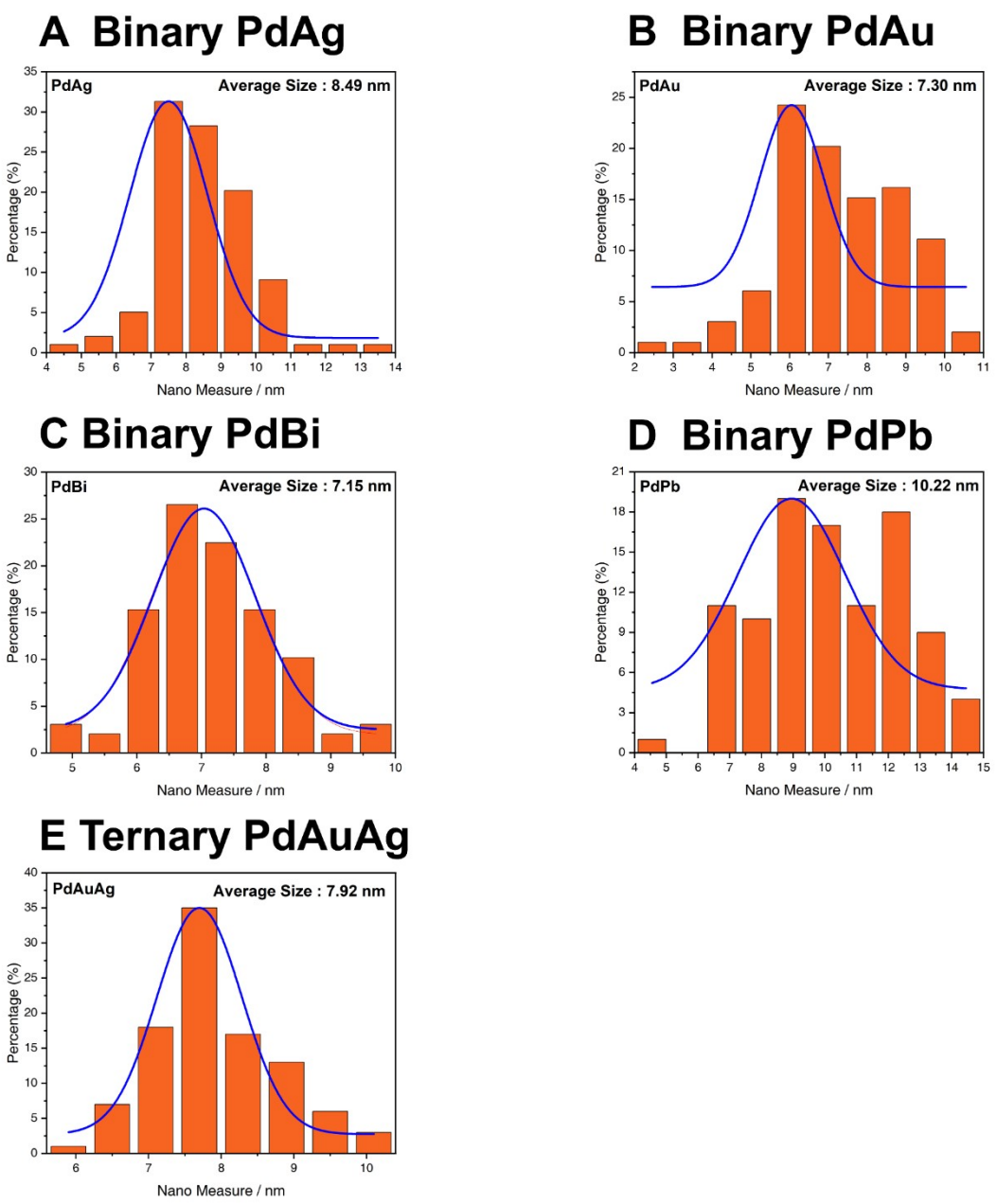

Figure S7. Statistical size distribution of (A) PdAg, (B) PdAu, (C) PdBi, (D) PdPb, and (E) PdAuAg nanoparticles.

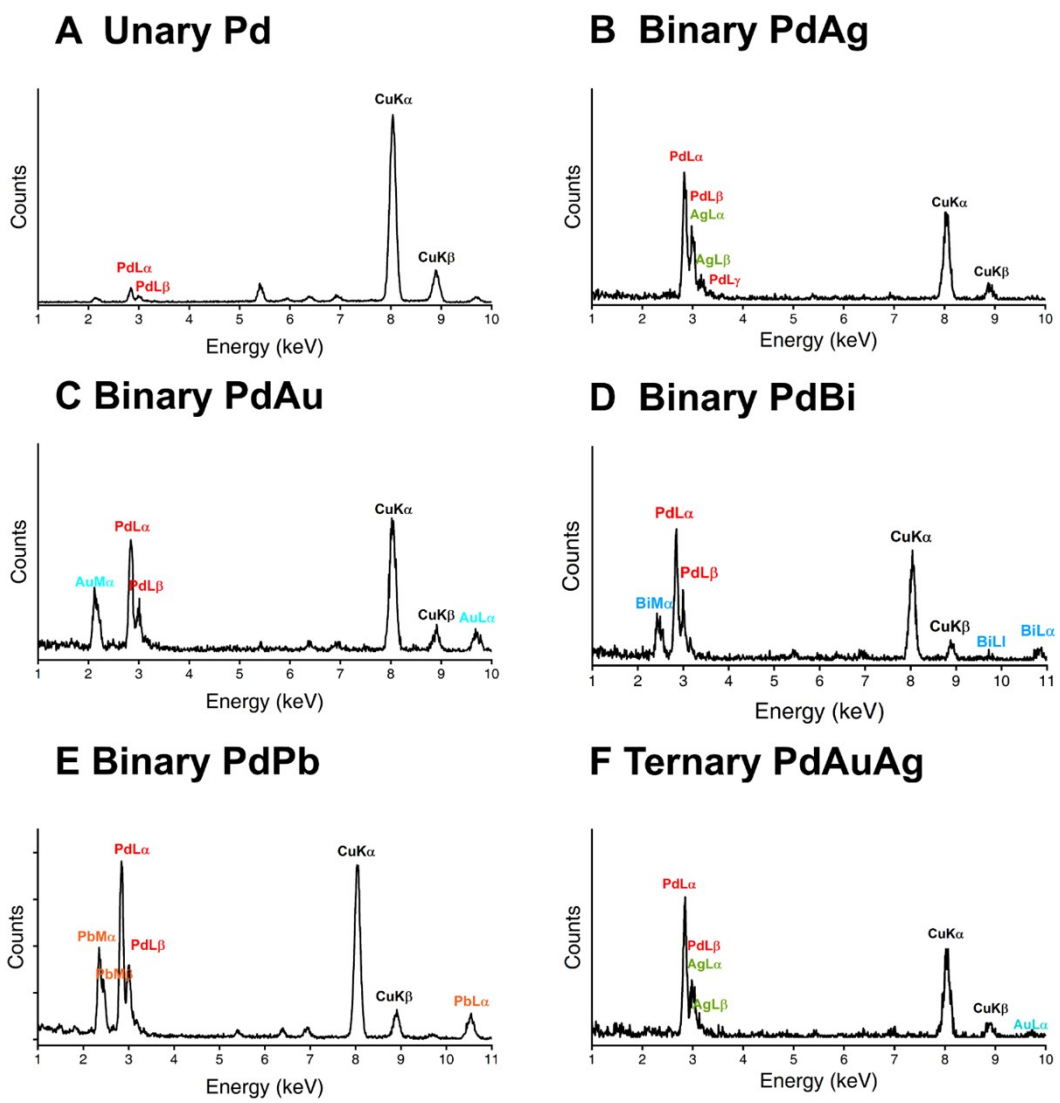

Figure S8. EDS spectra of (A) Pd, (B) PdAg, (C) PdAu, (D) PdBi, (E) PdPb, and (F) PdAuAg nanoparticles.

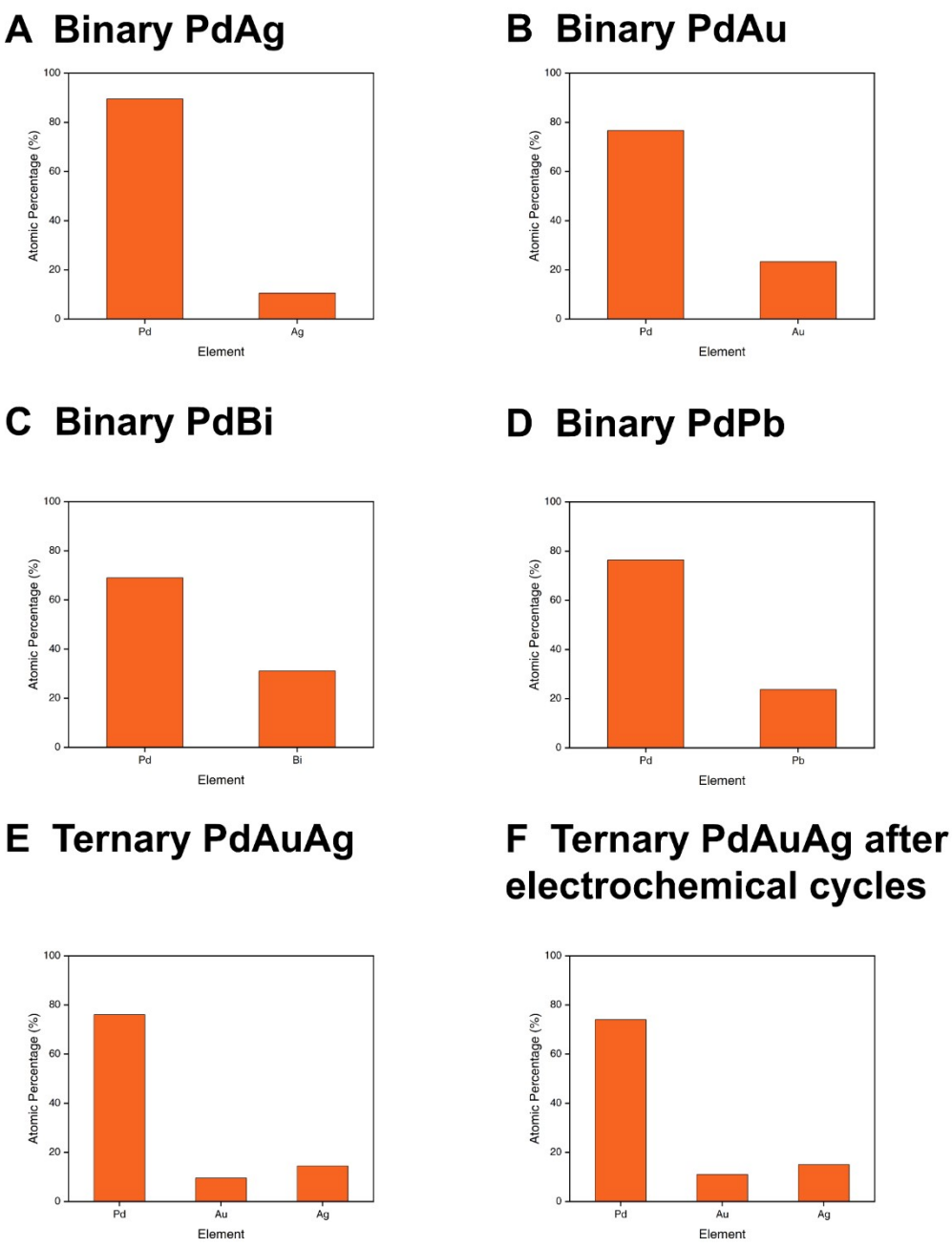

Figure S9. Atomic composition of (A) PdAg, (B) PdAu, (C) PdBi, (D) PdPb, and (E) PdAuAg nanoparticles. (F) Atomic composition of PdAuAg nanoparticles after electrochemical cycles.

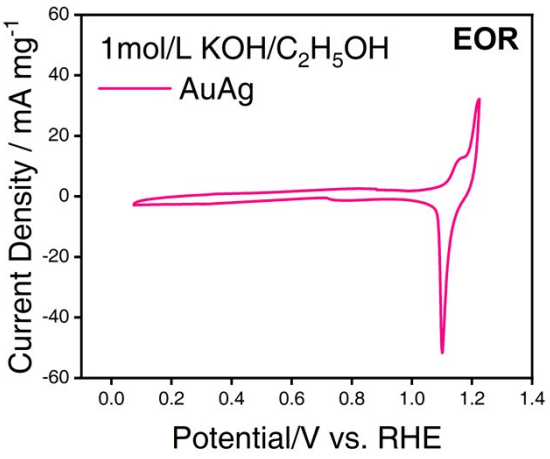

Figure S10. Electrocatalytic performance of AuAg nanoparticles.

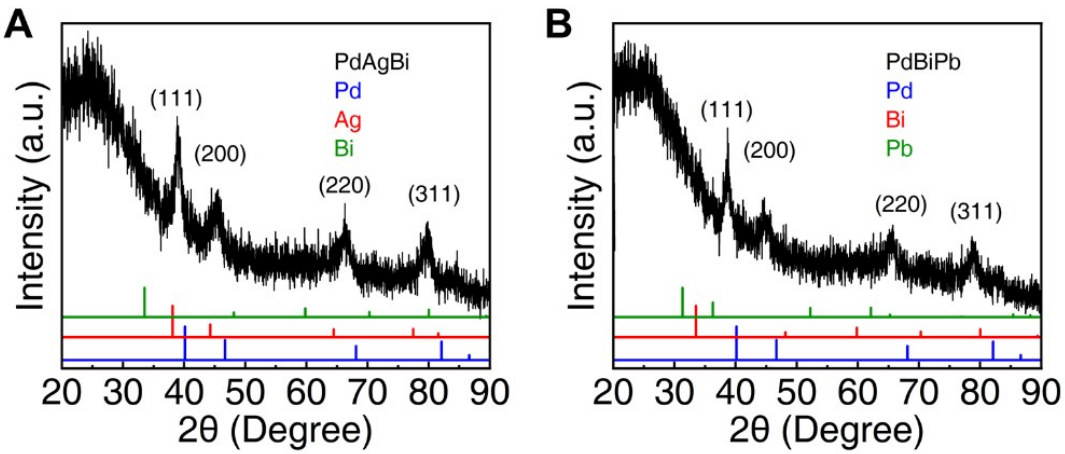

Figure S11. PXRD patterns of PdAgBi and PdBiPb nanoparticles.

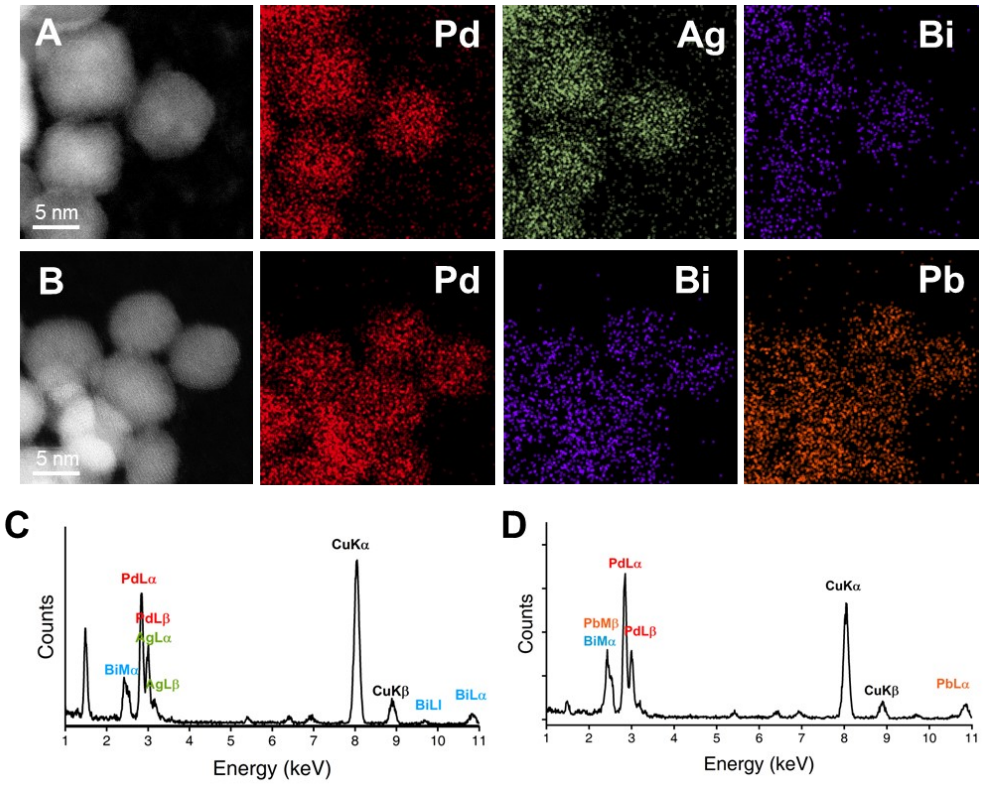

Figure S12. HAADF-STEM images and corresponding elemental mapping of (A) PdAgBi and (B) PdBiPb nanoparticles. EDS spectra of (C) PdAgBi and (D) PdAuAg nanoparticles.

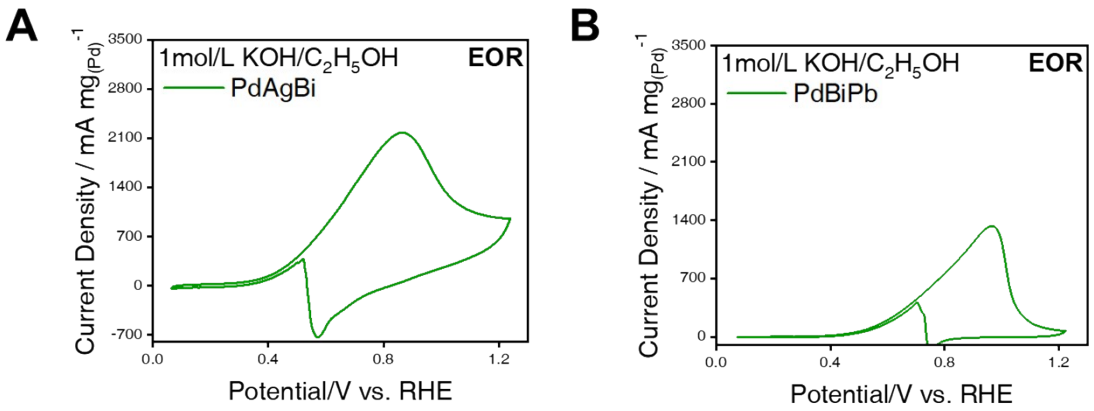

Figure S13. EOR CV curves of (A) PdAgBi and (B) PdBiPb nanoparticles.

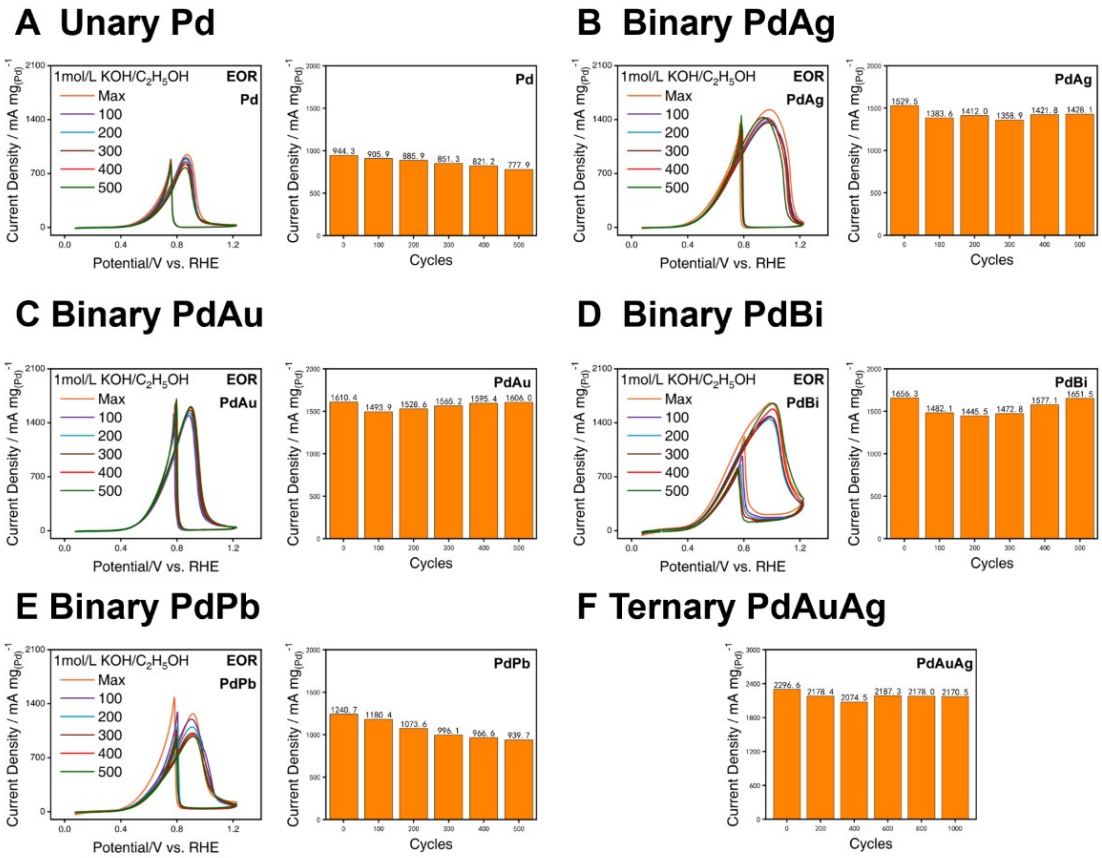

Figure S14. (A-E) Mass-normalized CV curves and (A-F) change of the current density of (A) Pd, (B) PdAg, (C) PdAu, (D) PdBi, (E) PdPb, (F) PdAuAg nanoparticles after cycling tests in 1.0M KOH/1.0M C_2H_5OH electrolyte.

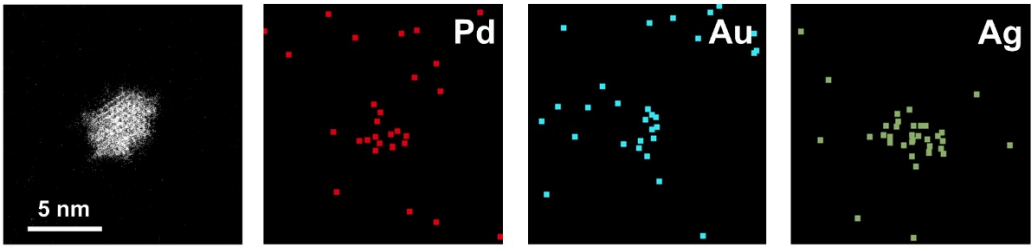

Figure S15. HAADF-STEM images and corresponding element mapping of PdAuAg nanoparticles after electrochemical cycles. After 1000 cycles of EOR test, the surface of PdAuAg nanoparticles is coated with nafion, ethanol, acetic acid, and other reaction species. These contaminants deteriorate the resolution of the EDS elemental mapping.

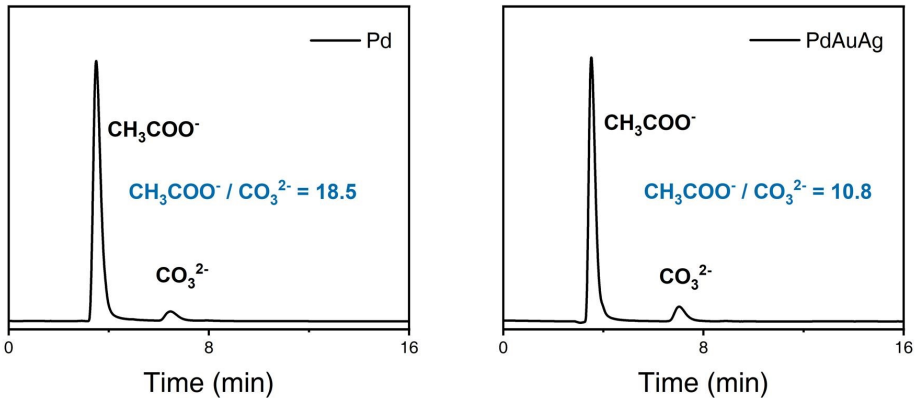

Figure S16. IC spectra of the electrolytes using Pd and PdAuAg nanoparticles as the catalysts showing the distribution of reaction products.

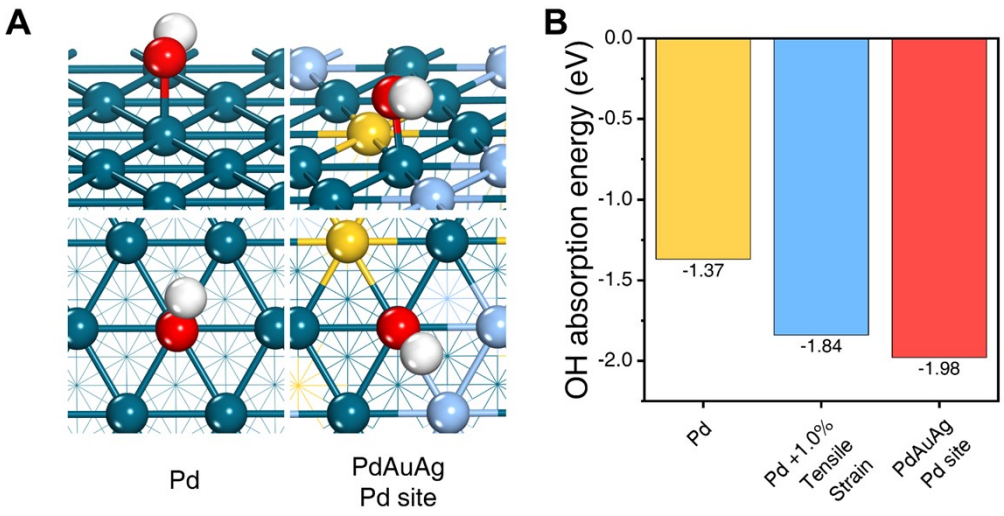

Figure S17. Schematic diagram and adsorption energy chart of OH adsorption on Pd (111) surfaces, Pd (111) +1.0% tensile-strained surface, and the Pd sites of the PdAuAg (111) surface.

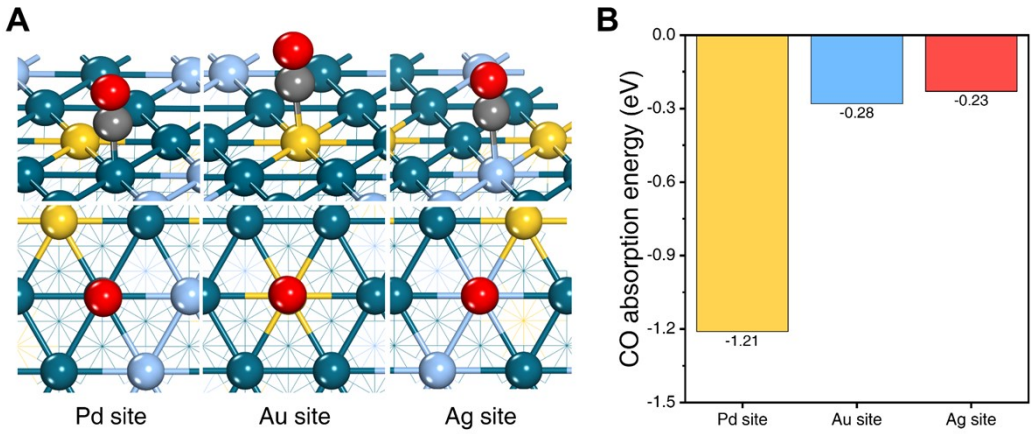

Figure S18. Schematic diagram and adsorption energy chart of CO adsorption on the Pd, Au, and Ag sites of PdAuAg (111) surface.

Table S1. Comparison of the mass activities of noble metal nanoarchitectures for EOR in an alkaline environment.

No.	Catalysts	Test conditions	Mass activity	Reference
1	PdAuAg NPs	1M KOH + 1M C_2H_5OH	2448.7 mA mg_{Pd}^{-1}	This work
2	Pd nanowire@crystalline Cu O_x	1M KOH + 1M C_2H_5OH	500 mA mg_{Pd}^{-1}	[1]
3	m-PtPb NSs	1M KOH + 0.1M C_2H_5OH	1233.7 mA mg_{Pd}^{-1}	[2]
4	PGM-HEA	1M KOH + 1M C_2H_5OH	~1600 mA $mg_{noble\ metals}^{-1}$	[3]
5	0.2SnO_2–Rh NSs/C	0.1M KOH + 0.5M C_2H_5OH	213.2 mA mg_{Rh}^{-1}	[4]
6	RhCuBi TMEs	1M KOH + 1M C_2H_5OH	1110 mA mg_{Rh}^{-1}	[5]
7	$Pd_{1.84}Sn@SnO_x$	1M KOH + 1M C_2H_5OH	495 mA mg_{Pd}^{-1}	[6]
8	PdInMo	1M KOH + 1M C_2H_5OH	2668.49 mA mg_{Pd}^{-1}	[7]

Table S2. Comparison of the mass activities of noble metal nanoarchitectures for EOR in an acidic environment.

No.	Catalysts	Test conditions	Mass activity	Reference
1	PtIrRhCoFeNiCu	0.1M $HClO_4$ + 0.5M C_2H_5OH	2130 mA mg_{Pt}^{-1}	[8]
2	$L_{10}Co_{41}Pt_{44}Au_{15}$NPs	0.1M $HClO_4$ + 2M C_2H_5OH	1233 mA mg_{Pt}^{-1}	[9]
3	Pt_3Sn nanofibers	0.1M $HClO_4$ + 0.5M C_2H_5OH	2150 mA mg_{Pt}^{-1}	[10]
4	$Pt_{74}Mn_{21}Ir_5$ NWs	0.1M $HClO_4$ + 0.5M C_2H_5OH	670 mA mg_{Pt}^{-1}	[11]
5	PtNiRh-E-H nanotubes	0.1 M $HClO_4$ + 0.5 M C_2H_5OH	1810 mA mg_{Pt}^{-1}	[12]
6	22% YO_X/MoO_X-Pt ultrathin nanowires	0.1M $HClO_4$ + 0.5M C_2H_5OH	1630 mA mg_{Pt}^{-1}	[13]
7	$Pt_{69}Ni_{16}Rh_{15}$ ultrathin nanowires	0.1M $HClO_4$ + 0.5M C_2H_5OH	1500 mA mg_{Pt}^{-1}	[14]

Table S3. Quantitative analysis of the current decay rate in CA tests.

Catalyst	Pd	PdAg	PdAu	PdBi	PdPb	PdAuAg
Current reaction rate (%)	76.4%	61.6%	66.0%	95.0%	57.7%	94.9%
Percentage of decay (%)	23.6%	38.4%	34.0%	5.0%	42.3%	5.1%
Average decay rate (μA mg_{Pd}^{-1} / sec)	2.36	3.84	3.40	0.50	4.23	0.51

Reference

[1] Z, Chen; Y, Liu; C, Liu; J, Zhang; Y, Chen; W, Hu; Y,Deng. Engineering the Metal/Oxide Interface of Pd Nanowire@CuO_x Electrocatalysts for Efficient Alcohol Oxidation Reaction. Small. 2020, 16, 1904964.

[2] W, Ao; H, Ren; C, Cheng; Z, Fan; P, Yin; Q, Qin; Q, Zhang; L, Dai. Mesoporous PtPb Nanosheets as Efficient Electrocatalysts for Hydrogen Evolution and Ethanol Oxidation. Angew. Chem. Int. Ed. 2023, 62, e202305158.

[3] D,Wu; K, Kusada; T, Yamamoto; T, Toriyama; S, Matsumura; S, Kawaguchi; Y, Kubota; H, Kitagawa. Platinum-group-metal High-entropy-alloy Nanoparticles. J. Am. Chem. Soc. 2020, 142, 13833-13838.

[4] S, Bai; Y, Xu; K, Cao; X, Huang. Selective Ethanol Oxidation Reaction at the Rh–SnO_2 Interface. Adv. Mater. 2021, 33, 2005767.

[5] F, Li; C. Xia; W, Fang; Y, Chen; B, Xia. RhCuBi Trimetallenes with Composition Segregation Coupled Crystalline-Amorphous Heterostructure Toward Ethanol Electrooxidation. Adv. Energy Mater. 2024, 14, 2400112.

[6] A, Chandran; S, Mondal; D, Goud; D, Bagchi; A, Singh; M, Riyaz; N, Dutta; S, C. Peter. In Situ Metal Vacancy Filling in Stable Pd-Sn Intermetallic Catalyst for Enhanced C–C Bond Cleavage in Ethanol Oxidation. Adv. Mater. 2025, 37, 2415362.

[7] Q, Guo; J, Dou; X, Yang; Z, Jiang; H, Wang; Y, Liu; H, Xie; X, Li. Construction of Multiphase Concave Tetrahedral PdInMo Nanocatalyst for Enhanced Alcohol Oxidation. Adv. Funct. Mater. 2025, 35, 2413937.

[8] Y, Wang; H, Meng; R, Yu; J Hong; Y, Zhang; Z, Xia; Prof. Yong Wang. Unconventional Interconnected High-Entropy Alloy Nanodendrites for Remarkably Efficient C−C Bond Cleavage toward Complete Ethanol Oxidation. Angew. Chem. Int. Ed. 2025, e202420752 .

[9] J, Li; S, Z. Jilani; H, Lin; X, Liu; K, Wei; Y, Jia; P, Zhang; M, Chi; Y, J. Tong; Z, Xi; S, Sun; Ternary CoPtAu Nanoparticles as a General Catalyst for Highly Efficient Electro-oxidation of Liquid Fuels. Angew. Chem. Int. Ed. 2019, 58, 11527-11533.

[10] Y, Zhu; L, Bu; Q, Shao; X, Huang. Structurally Ordered Pt_3Sn Nanofibers with Highlighted Antipoisoning Property as Efficient Ethanol Oxidation Electrocatalysts. ACS Catal. 2020, 10, 3455-3461.

[11] F, Gao; Y, Zhang; F, Ren; T, Songa; Y, Du. Tiny Ir Doping of Sub-one-nanometer PtMn Nanowires: Highly Active and Stable Catalysts for Alcohol Electrooxidation. Nanoscale. 2020, 12, 12098–12105.

[12] Z, Xia; R, Yu; Y, Wang; K, Xu; K, Eid; Y, Zhang; J, He; F, Ning; L, Liu; J, Zhang; H, Yang; H, Zhao; D, Zhang. Cavities-Induced Compressive Strain in Unique Nanotubes Boosts the C_1 Pathway of Ethanol Oxidation Electrocatalysis. ACS Nano 2025, 19, 7379−7390.

[13] M, Li; Z, Zhao; W, Zhang; M, Luo; L, Tao; Y, Sun; Z, Xia; Y, Chao; K, Yin; Q, Zhang; L, Gu; W, Yang; Y, Yu; G, Lu; S, Guo. Sub-Monolayer YO_x/MoO_x on Ultrathin Pt Nanowires Boosts Alcohol Oxidation Electrocatalysis. Adv. Mater. 2021, 33, 2103762.

[14] W, Zhang; Y, Yang; B, Huang; F, Lv; K, Wang; N, Li; M, Luo; Y, Chao; Y, Li; Y, Sun; Z, Xu; Y, Qin; W, Yang; J, Zhou; Y, Du; D, Su; S, Guo. Ultrathin PtNiM (M = Rh, Os, and Ir) Nanowires as Efficient Fuel Oxidation Electrocatalytic Materials. Adv. Mater. 2019, 31, 1805833.